Journal of Organometallic Chemistry 882 (2019) 64–69

Contents lists available at ScienceDirect

Journal of Organometallic Chemistry

journal homepage: www.elsevier.com/locate/jorganchem

Synthesis of decorated carbon nanotubes with Fe_3O_4 and Au nanoparticles and their application in catalytic oxidation of alcohols in water

Babak Kaboudin [a, b, *], Fatemeh Saghatchi [a], Foad Kazemi [a]

[a] Department of Chemistry, Institute for Advanced Studies in Basic Sciences (IASBS), Gava Zang, Zanjan, 45137-66731, Iran
[b] Center for Research in Basic Sciences and Contemporary Technologies, Institute for Advanced Studies in Basic Sciences (IASBS), Gava Zang, Zanjan, 45137-66731, Iran

ARTICLE INFO

Article history:
Received 15 October 2018
Received in revised form
30 November 2018
Accepted 15 December 2018
Available online 18 December 2018

Keywords:
Carbon nanotubes
Magnetic nanoparticles
Gold nanoparticles
Alcohol oxidation

ABSTRACT

Magnetic decorated multi-walled carbon nanotubes (*m*-MWCNTs) were functionalized using 4-aminopyridine to introduce pyridine groups on the carbon nanotubes (*mf*-MWCNTs). The pyridine functionalized magnetic decorated multi-walled carbon nanotubes were used as a support for gold nanoparticles. A thorough structural characterization has been carried out by means of transmission electron microscopy (TEM), scanning electron microscopy (SEM) images, EDS, CHN and spectroscopy. The *mf*-MWCNTs supported gold nanoparticles were found to be an efficient catalyst for the oxidation of alcohols in water.

1. Introduction

Hybrid composite materials, incorporating metal and metal oxide nanoparticles, have attracted much attention due to their uses in photonic crystal, surface-enhanced Raman scattering and plasmon resonance [1–5]. Amongst the various materials that are used for the fabrication of metal nanoparticles, carbon nanotubes have attracted much attention [6–8]. Carbon nanotubes are sheets of six-membered carbon atom rings rolled up into cylinders which one layer are known as single-walled CNTs (SWCNTs) and with two-walls CNTs (DWCNTs) and more layers are known as multi-walled CNTs (MWCNTs). MWCNTs is one of the most used carbon nanostructures due to its easy availability, affordable price, chemical inertness and ability to be functionalized easily. More significantly, MWCNTs have large surface area with high reactivity which can be covalently modified with functional groups such as thiols, phosphines, carboxylic acids and amines that results in their ability to be decorated with metal nanoparticles [9,10]. Magnetic nanoparticles (MNPs) have attracted much attention due to their uses in immobillization of cells and enzymes, magnetic resonance imaging and thermotheraputic agents for the diagnosis of many diseases, gene and drug delivery [11–15]. The magnetic properties of MNPs allow the remote control of their accumulation by means of an external magnetic field and coupling with drugs, poroteins and nucleic acids, in combination with an external magnetic field to target the nanoparticles has additionally emerged as a promising strategy of delivery [23].

Gold nanoparticles have been in focus of both academic and industrial research in the past few decades due to their unique properties in various fields ranging from catalysis, electrocatalysis and optical kits for cancer therapy and drug delivery [16–22]. The fabrication of gold nanoparticles on colloidal carbon nanotubes can be achieved in a number of various methods such as electrodeposition, chemical decoration $\pi-\pi$ stacking, sonochemistry, wet impregnation and other means which a chemical reduction is most commonly and convenient [24–26].

In contrast to the widely studied gold nanoparticles coated on various functionalized materials [27], relatively few papers have been reported on the preparation of controlled size of nano gold particles on simple functionalized carbon nanotubes [28–30], although there is evidence that these nanocomposites are applicable in oxidation reaction of alcohols [31–33]. Pratia and co-

* Corresponding author. Department of Chemistry, Institute for Advanced Studies in Basic Sciences (IASBS), Gava Zang, Zanjan, 45137-66731, Iran.
E-mail address: kaboudin@iasbs.ac.ir (B. Kaboudin).

https://doi.org/10.1016/j.jorganchem.2018.12.012
0022-328X/

workers reported liquid phase oxidation of alcohols by a nitrogen functionalized CNT prepared by dierct amination of CNT with ammonia gas for the supporting of Au-Pd nanoparticles [31]. Recently a self-assembly of amphiphilic nitrilotriacetic-diyne lipid on CNT has been reported by Doris and co-workers for the synthesis of novel carbon nanotube-gold nanohybride catalyst for oxidation of alcohols [32]. More recently, Wang and co-workers reported preparation and applications of gold nanoparticles loaded on nitric acid-pretreated carbon nanotubes for the selective oxidation of cellobiose by molecular oxygen to gluconic acid in aqueous medium at 145 °C [33].

In this study, we report preparation and characterization of a novel pyridine functinalized magnetic carbon nanotubes supported gold nanoparticles. The magnetic CNT supported gold nanoparticles was also applied as a catalyst for the aerobic oxidation of alcohols in water.

2. Materials and methods

2.1. Oxidative treatment of MWCNTs

The commercial MWCNTs (CAS: 308068-56-6 from Aldrich O.D.xL = 6–9 nm x 5 μm, Fig. 1 shows TGA of MWCNTs) were oxidized according to the literature by stirring the MWCNT in concentrated nitric acid at 60 °C for 12 h [34].

2.2. Preparation of Fe_3O_4/MWCNTs (m-MWCNTs)

The magnetic nanoparticle composite of Fe_3O_4/MWCNTs was prepared according to our recently report and the literature with slight modification [23,35]. Oxidized MWCNTs (1.0 g) was added to a solution mixture of $(NH_4)_2Fe(SO_4)\cdot 6H_2O$ (1.7 g, 4.33 mmol) and $NH_4Fe(SO_4)_2\cdot 12H_2O$ (2.51 g, 8.66 mmol) in water (200 mL) at 50 °C under N_2 atmosphere. The solution was sonicated for 10 min and then NH_4OH (10 mL, 8 M) was added dropwise to precipitate the iron oxides while the mixture solution was sonicated. The pH of the final mixture should be in the range of 11–12. The precipitate was isolated by an external magnet and the supernatant was separated from the precipitate by decantation. Fe_3O_4/MWCNTs were washed with doubly distilled water (500 mL). The obtained Fe_3O_4/MWCNTs nanocomposite (*m*-MWCNTs) was then washed with absolute alcohol (150 mL) for three times and then dried under vacuum.

2.3. Pyridine functionalized m-MWCNTs (mf-MWCNTs)

$NaNO_2$ (0.490 g, 7.10 mmol) was dissolved in water (0.7 mL) and added dropwise to a cooled solution of 4-aminopyridine (0.658 g, 6.99 mmol) in HCl (5 mL, 4 M). The resulting solution was stirred for 30 min at 0 °C. The soultion was added to a sonicaed dispersed mixture of *m*-MWCNTs (20 mg) in DMF (20 mL) and the mixture was stirred for 4 h at 0 °C and 15 h at room temperature. The precipitate was isolated by external magnet and the supernatant was separated from the precipitate by decantation. The solid was dispersed in HCl (100 mL, 2 M) and again isolated by external magnet and the composite was washed with water (500 mL). The resulting solid material was dispersed in NaOH (100 mL, 2 M) and stirred overnight to ensure deprotonation of the pyridinium salt to free pyridine and the *mf*-MWCNT composite was then isolated by an external magnet, washed with water, THF (2 × 30 mL), acetone (2 × 30 mL), and ethanol (2 × 30 mL), respectively. The composite dried overnight at 80 °C to afford purified *mf*-MWCNT [36,37].

2.4. Preparation of mf-MWCNTs stabilized gold nanoparticles (AuNPs/mf-MWCNT)

To an aqueous solution of $HAuCl_4$ (1 mM, 35 mL) was added 14 mg of *mf*-MWCNT. The mixture was stirred for 30 min at 0 °C. Then, an aqueous solution of $NaBH_4$ (100 mM, 5 mL) was rapidly sprayed into the reaction mixture with a syringe under vigorous stirring. The mixture was further stirred for 1 h. The precipitate AuNPs/*mf*-MWCNT was isolated in the magnetic field, and the supernatant was separated from the precipitate by decantation. The AuNPs/*mf*-MWCNT were subsequently washed with deionized water to remove inorganic impurities. The composite was dispersed and isolated by the magnetic field in ethanol and dried overnight at 80 °C [38].

2.5. Oxidation of benzyl alcohol catalysed by AuNPs/mf-MWCNT

AuNPs/*mf*-MWCNT (3 mg, 1.88 mmol Au/g catalyst) in distilled water (2 mL) was dispersed for 5 min by ultrasound. K_2CO_3 (0.08 g, 0.6 mmol) and benzyl alcohol (20 μL, 0.2 mmol) was added into the reaction mixture and the mixture was stirred under an atmospheric of oxygen for 16 h at 50 °C. The catalyst were collected by external magnet and washed three times with deionized water. The solution

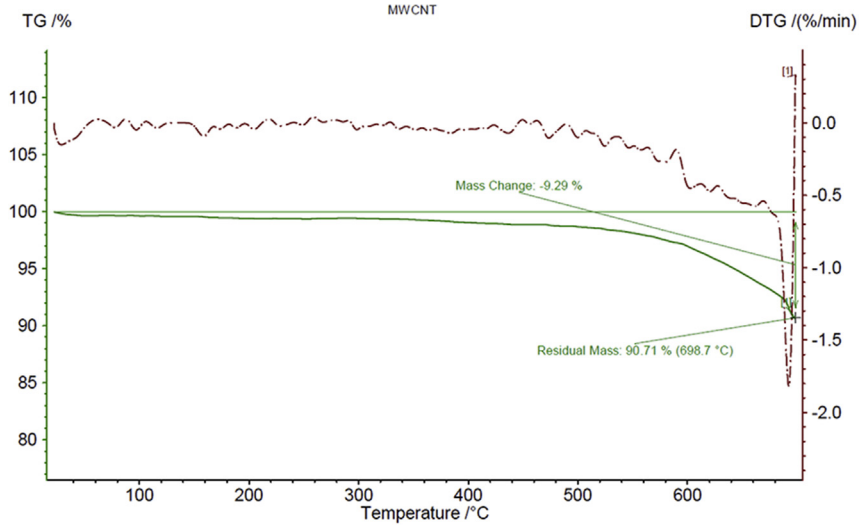

Fig. 1. TGA of MWCNT composite.

was neutralized with 0.1 M HCl (pH = 3–4) and extracted with AcOEt (3 × 7 mL). The extracted organic layer was dried over Na_2SO_4 and then analyzed by gas chromatography. The GC yield was obtained from the calibration curve.

3. Results and discussion

Pyridine groups through lone-pair on their nitrogen atoms and also benzene ring in MWCNTs are ideal stabilizers for gold nanoparticles [31,39]. Although gold has been reported as a poor catalytic metal, its nanosized in nanocomposites have been shown to be able to catalyze chemical transformations [40–42]. The preaparation of magnetic CNTs opens new possibilities in nanotechnology applications [43]. Therefore we decided to prepare pyridine functionalized magnetic decorated MWCNTs to synthesize gold nanoparticles on their surface. Scheme 1 shows a schematic illustration of the step-by-step approch for the preparation of AuNPs/*mf*-MWCNT.

The magnetic nanoparticles of MWCNTs (*m*-MWCNTs) heterostuctures were achieved by the co-precipitating of iron metal ions within a dispersion of MWCNTs [35]. In order for the functinalization of *m*-MWCNTs with pyridine groups, aryldiazonium salts were found as a convenient precursor [36]. Therefore, the next step (pyridine functinalization) was achieved by direct reaction of the *m*-MWCNTs with 4-pyridinediazonium salt.

The functional groups of nanomaterials were characterized by FT-IR spectroscopy (Fig. 2). Fisrt of all, the vibration band of Fe-O appeared at 540-700 cm^{-1} wave number range. The pyridine groups of *mf*-MWCNTs were measured at about 1600–1700 cm^{-1} wave number range. The assignments for *mf*-MWCNTs are concordant with the Tuci reported on pyridine functionalized CNTs [36]. Therefore by FT-IR analysis, it can be concluded that Fe_3O_4 nanoparticles and pyridine groups have been bonded successfully on the surface of MWCNTs.

AuNPs/*mf*-MWCNT were preapred by sonication of *mf*-MWCNTs in distilled water, followed by the addition of $HAuCl_4{\cdot}3H_2O$ aqueous solution and treatment with ice-cooled $NaBH_4$ solution, as a reductant, at room temperature with vigorous stirring for 1 h.

The morphology and structure of the prepared AuNPs/*mf*-MWCNT was characterized by SEM, TEM, EDS, XRD and atomic absorption analyses, which confirmed the successful preparation of AuNPs/*mf*-MWCNT.

The SEM image of the AuNPs/*mf*-MWCNT is shown in Fig. 3. Fig. 3 shows the CNT nanowires decorated with Fe_3O_4 and Au nanoparticles.

Also, elemental analysis for *m*-MWCNTs and *mf*-MWCNT confirm successfully attachment of pyridine and Fe_3O_4 groups on *mf*-MWCNTs. The elemental analysis of *mf*-MWCNTs showed that the C/N and C/Fe ratio is 115/1 and 28/1 respectively. The content of Au in AuNPs/*mf*-MWCNT was measured by atomic absorption spectrometry (1.87 mmol of Au per 1 g of the catalyst). The elemental analysis (EDS) confirmed the presence of Au, Fe, and N in the nanocomposite (Fig. 3). EDS quantitative microanalysis indicates that the nanocomposite has a composition of Au, Fe, O, N, and C.

TEM was used to obtain direct information about the structure and morphology of novel composite. Fig. 3 shows the TEM image of prepared AuNPs/*mf*-MWCNT. In TEM, black dots indicate Au NPs and pale gray dots indicate iron oxide NPs [44]. TEM showed that the mean diameter of Au nanaoparticles is about 15 nm.

In the XRD spectrum of AuNPs/*mf*-MWCNT (Fig. 4), all diffraction peaks and positions match well with those from the JCPDS card (No. 01–1172) for the faced-centered cubic gold and cubic Fe_3O_4 (JCPDS card no. 75–0449) on the surface of *mf*-MWCNTs. The average crystallite sizes of Fe_3O_4 nanoparticles estimated using Scherrer's equation is ~23 nm. Comparing the XRD spectrum of AuNPs/*mf*-MWCNT with XRD of *m*-MWCNT [23], showed that the Au nanoparticles decoreted on the surface of MWCNT. The average crystallite sizes of Au nanoparticles estimated using Scherrer's equation is ~18 nm for AuNPs/*mf*-MWCNT.

Catalytic oxidation of alcohols using oxygen as oxidant in water in the presence of recyclable and reusable gold supported catalysts, is one of the most economical and environmental-friendly advanced oxidation process [45–47]. The catalytic oxidation activity of the nanocomposite was assessed using benzyl alcohol as a model compound under an atmospheric of oxygen. Since reported analogous supported gold nanoparticles for the oxidation of alcohols usually require reaction conditions such as heating and oxygen pressure, in a preliminary screening, oxidation of benzylalcohol (0.2 mmol) in the presence of AuNPs/*mf*-MWCNT catalyst (3 mg) in water (2 mL) was performed under an atmospheric of oxygen at room temperature. The results showed that after 24 h no products (benzaldehyde or benzoeic acid) were observed (Table 1 entry 1). The conversion proceeded to only 40% with the addition of certain base (K_2CO_3, 3 equiv) to the reaction mixture at room temperature. The conversion increased to 100% with increasing the reaction temperature to 50 °C (entries 2–4). By screening of different bases (3 equiv) we found that K_2CO_3 was the best (entries 5–9). The oxidation reaction catalyzed by AuNPs/*mf*-MWCNT in the presence of K_2CO_3 is highly selective to benzoic acid, found as the sole product (entry 4). When the oxidation reaction was performed under an aerobic condtion at 50 °C, the conversion was decreased to 16% (Table 1, entry 12). Hydroxide ions play an important role during oxidation and no activity is seen over Au catalysts without

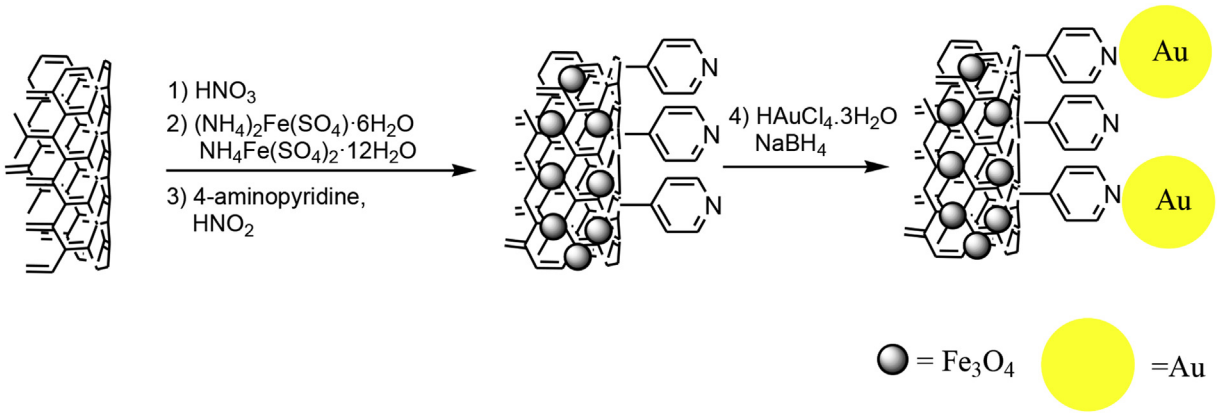

Scheme 1. Schematic illustration of the step-by-step approch for the preparation of AuNPs/*mf*-MWCNT.

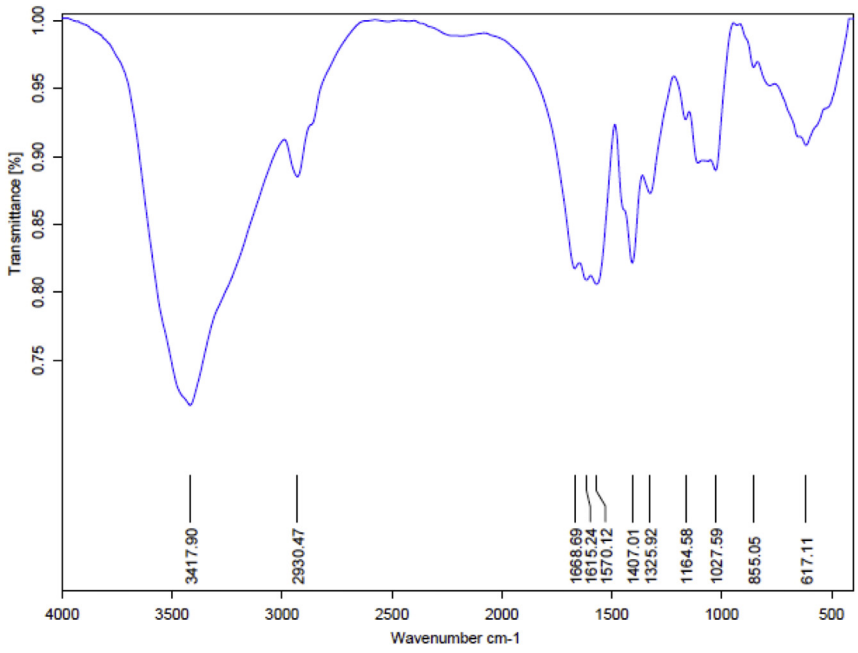

Fig. 2. FT-IR spectrums of *mf*-MWCNTs.

SEM TEM

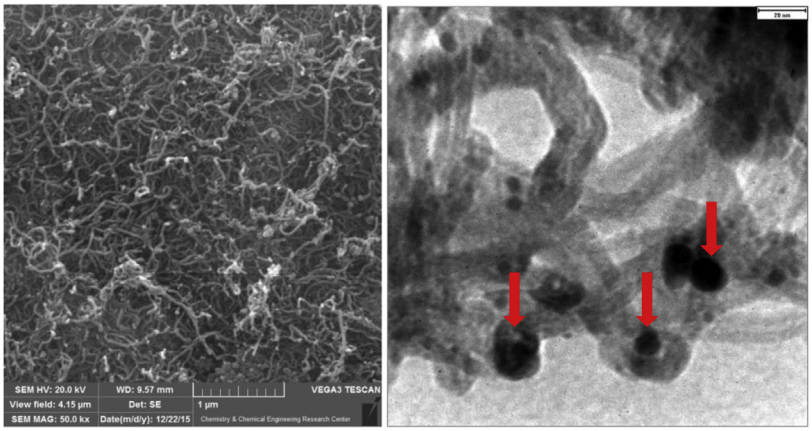

EDS

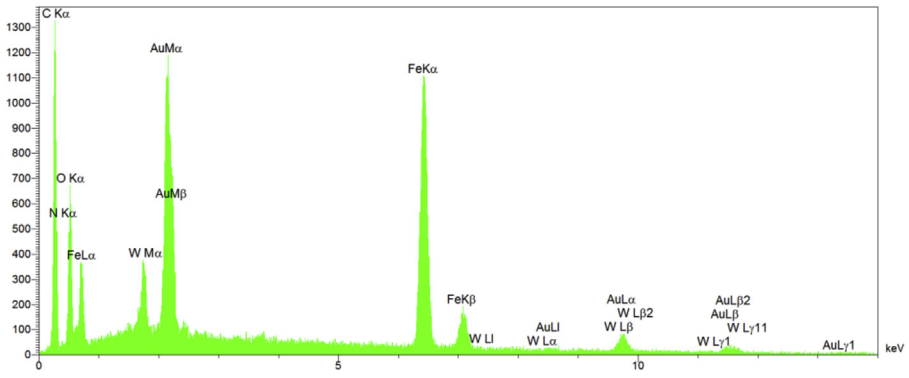

Fig. 3. The SEM, EDS and TEM of AuNPs/*mf*-MWCNT

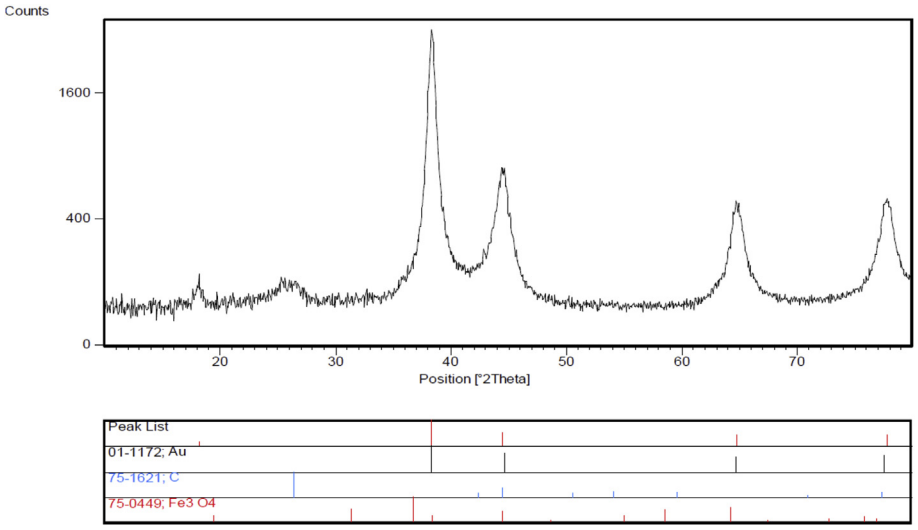

Fig. 4. XRD from AuNPs/*mf*-MWCNT composite.

Table 1
Oxidation of benzyl alcohol by AuNPs/*mf*-MWCNT composite.

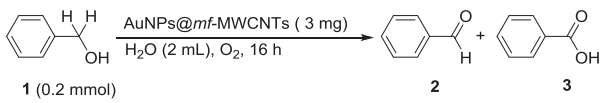

Entry	Base[a]	Temperature (°C)	Conversion (%)[b]	Selectivity (%)[b]	
				2	3
1	–	25	0	0	0
2	K_2CO_3	25	40	8	32
3	K_2CO_3	40	60	10	50
4	K_2CO_3	50	100	–	100
5	Cs_2CO_3	50	16	4	12
6	Na_2CO_3	50	–	–	–
7	KOH	50	98	–	98
8	NaOH	50	24	5	19
9	$N(Et)_3$	50	–	–	–
10	K_2CO_3[c]	50	9	6	3
11	K_2CO_3[d]	50	68	2	66
12	K_2CO_3[e]	50	16	7	9

[a] Reaction condition: 0.6 mmol base under O_2.
[b] Conversion and selectivity determined by GC.
[c] 0.3 mmol of K_2CO_3.
[d] 2 mg of AuNPs/*mf*-MWCNT.
[e] Oxidation reaction under an aerobic condition.

adding a base (Table 1 entry 1). The mechanism of the over-oxidation of benzyl alcohol to benzoic acid was occurred *via* the formation of the gem-benzidiol $PhCH(OH)_2$ intermediate [48]. On the other hand, for Au catalysts, particle size and support composition had negligible effect on the rate or selectivity of the oxidation reactions [49].

The recyclability and reusability are very important points for heterogeneous catalysis systems. The recycling experiments were examined for the catalytic oxidation of benzyl alcohol under an atmospheric of oxygen at 50 °C in the presence of K_2CO_3 as a base. After the first run, the catalyst were collected by external magnet and washed three times with deionized water. The catalyst were reused without significant loss of activity. Atomic absorption analysis of recovered catalyst showed that Au amount decreased to 1.7 mmol of Au per gram of the catalyst after fifth run. Results showed a negligible Au leaching occurred after fifth run from the catalyst.

Using the new nanocomposite described here convertion yield for the oxidation of 1-heptanol is excellent with quantitatively yield and slectivity achived for the desired acid product (Scheme 2). Such selectivity and efficacy is far superior to other AuNPs supported on CNTs catalysts (For example Doris and co-workers reported yield of only <5% for aliphatic alcohols [32]).

To further extend the scope of the reaction, secondary alcohol 1-phenyl ethanol was also studied under similar condtions. 1-Phenyl ethanol was also oxidized to the corresponding ketone with 100% yield (Scheme 2).

Interestingly, no reaction occurred under inert atmosphere of N_2 with both benzyl alcohol and 1-phenyl ethanol. The results showed that the oxidation reaction needs the molecular oxygen as an activator. Moreover, the conversion of the oxidation reaction of benzyl alcohol in THF was decreased to 25% and the major product was benzaldehyde(17%). Thus the presented catalytic system has selectivity depending on the reaction conditions.

4. Conclusions

We reported here a successful preparation of novel functionalized MWCNTs containing gold nanoparticles. Transmission electron microscopy (TEM), scanning electron microscopy (SEM) images, XRD and EDS analysis confirmed that the Au nanoparticles were successfully immobilized on the *mf*-MWCNTs. This novel composite exhibited a catalytic activity in the oxidation reaction of benzyl alcohol with less selectivity for the benzaldehyde product. The catalyst was also applicable for the oxidation of 1-phenyl ethanol, as a secondary alcohol, to acetophenone in high yield. The catalyst are efficiently recovered and reused for next run with negligible gold leaching to solution.

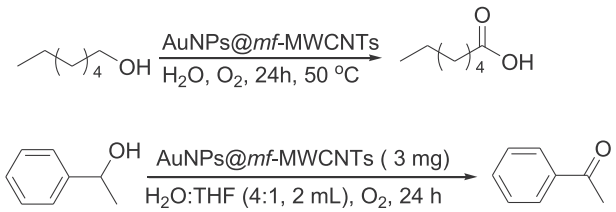

Scheme 2. Oxidation of heptanol and 1-phenylethanol catalysed by AuNPs/*mf*-MWCNT.

Acknowledgements

This work was supported by The Iran National Science Foundation (96003358). The authors also gratefully acknowledge for partial support by the Institute for Advanced Studies in Basic Sciences.

References

[1] X. Huang, C. Tan, Z. Yin, H. Zhang, Adv. Mater. 26 (2014) 2185–2204.
[2] C. Tan, H. Zhang, Chem. Soc. Rev. 44 (2015) 2713–2731.
[3] M.D. Xiao, H.J. Chen, T.A. Ming, L. Shao, J.F. Wang, ACS Nano 4 (2010) 6565.
[4] Z. Zhang, S.Q. Liu, Y.J. Xu, Nanoscale 4 (2012) 2227–2238.
[5] Y.G. Kim, W.-K. Jo, Int. J. Hydrogen Energy 42 (2017) 11356–11363.
[6] M. Sireesha, V.J. Babu, S. Ramakrishna, Mater. Sci. Eng. B 223 (2017) 43–63.
[7] N.D.Q. Chau, C. Menard-Moyon, K. Kostarelos, A. Bianco, Biochem. Biophys. Res. Commun. 468 (2015) 454–462.
[8] M. Xu, T. Liang, M. Shi, H. Chen, Chem. Rev. 113 (2013) 3766–3798.
[9] B. Wu, Y. Kuang, X. Zhang, J. Chen, Nano Today 6 (2011) 75–90.
[10] F. Fuchs, A. Zienert, C. Wagner, J. Schuster, S.E. Schulz, Microelectron. Eng. 137 (2015) 124–129.
[11] R. Tietze, J. Zaloga, H. Unterweger, S. Lyer, R.P. Friedrich, C. Janko, M. Pottler, S. Durr, C. Alexiou, Biochem. Biophys. Res. Commun. 468 (2015) 463–470.
[12] M. Aruebo, R. Fernandez-Pacheco, M.R. Ibara, J. Santamaria, Nano Today 2 (2007) 22–32.
[13] L. Mohammad, H.G. Gomaa, D. Ragab, J. Zhu, Particuology 30 (2017) 1–14.
[14] B. Kaboudin, A. Ghaderian, App. Sur. Sci. 282 (2013) 396–399.
[15] Z. Hedayatnasab, F. Abnisa, W.M.A.W. Daud, Mater. Des. 123 (2017) 174–196.
[16] B.S. Takale, M. Bao, Y. Yamamoto, Org. Biomol. Chem. 12 (2014) 2005–2027.
[17] M. Stratakis, H. Garcia, Chem. Rev. 112 (2012) 4469–4506.
[18] A. Majdalawieh, M.C. Kanan, O. ElKadri, S.M. Kanan, J. Nanosci. Nanotechnol. 14 (2014) 4757–4780.
[19] X. Liu, L. He, Y. Liu, Y. Cao, Acc. Chem. Res. 47 (2013) 793–804.
[20] F. Yang, C. Wang, L. Wang, C. Liu, A. Feng, X. Liu, C. Chi, X. Jia, L. Zhang, Y. Li, RSC Adv. 5 (2015) 37710–37715.
[21] Y.-C. Yeh, B. Creran, V.M. Rotello, Nanoscale 4 (2012) 1871–1880.
[22] B. Kaboudin, H. Khanmohammadi, F. Kazemi, App. Sur. Sci. 425 (2017) 400–406.
[23] B. Kaboudin, F. Saghatchi, F. Kazemi, S. Akbari-Birgani, ChemistrySelect 3 (2018) 6743–6749.
[24] A. Corma, H.S. Garcia, Chem. Soc. Rev. 37 (2008) 2096–2126.
[25] T. Liu, F. Yang, Y. Li, L. Ren, L.Q. Zhang, K. Xu, X. Wang, C. Xu, J. Gao, J. Mater. Chem. 2 (2014) 245–250.
[26] M. Cittadini, M. Bersani, F. Perrozzi, L. Ottaviano, W. Wlodarski, A. Martucci, Carbon 69 (2014) 452–459.
[27] L.M. Kustov, Russ. Chem. Bull. 62 (2013) 869–877.
[28] S. Orlanducci, D. Sordi, E. Tamburri, M.L. Terranova, J. Nanosci. Nanotechnol. 11 (2011) 4882–4887.
[29] J. Lee, M. Morita, K. Takemura, E.Y. Park, Biosens. Bioelectron. 102 (2018) 425–431.
[30] R.Y. Zhang, H. Olin, Int. J. Biomed. Nanosci. Nanotechnol. (IJBNN) 2 (2011) 112–135.
[31] A. Villa, D. Wang, P. Spontoni, R. Arrigo, D.S. Su, L. Pratia, Catal. Today 157 (2010) 89–93.
[32] R. Kumar, E. Gravel, A. Hagege, H. Li, D.V. Jawale, D. Verma, I.N.N. Namboothiri, E. Doris, Nanoscale 5 (2013) 6491–6497.
[33] X. Tan, W. Deng, M. Liu, Q. Zhang, Y. Wang, Chem. Commun. 0 (2009) 7179–7181.
[34] S. Qu, J. Wang, J. Kong, P. Yang, G. Chen, Talanta 71 (2007) 1096–1102.
[35] L. Gao, L. Chen, Microchimica Acta 180 (2013) 423–430.
[36] G. Tuci, C. Zafferoni, A. Rossin, A. Milella, L. Luconi, M. Innocenti, L.T. Phuoc, C. Duong-Viet, C. Pham-Huu, G. Giambastiani, Chem. Mater. 26 (2014) 3460–3470.
[37] H. Tsunoyama, H. Sakurai, N. Ichikuni, Y. Negishi, T. Tsukuda, Langmuir 20 (2004) 11293–11296.
[38] K. Jiang, A. Eitan, L.S. Scadler, P.M. Ajayan, R.W. Siegel, Nano Lett. 3 (2003) 275.
[39] M.K. Bayazit, L.S. Clarke, K.S. Coleman, N. Clarke, J. Am. Chem. Soc. 132 (2010) 15814–15819.
[40] A.S.K. Hashmi, G.J. Hutchings, Angew. Chem. Int. Ed. 45 (2006) 7896.
[41] Y. Mikami, A. Dhakshinamoorthy, M. Alvaro, H. Garcia, Catal. Sci. Technol. 3 (2013) 58.
[42] S. Carrettin, M. Carmen Blanco, A. Corma, A.S.K. Hashmi, Adv. Synth. Catal. 348 (2006) 1283.
[43] A. Masotti, A. Caporali, Int. J. Mol. Sci. 14 (2013) 24619–24642.
[44] J. Lee, S. Mulmi, V. Thangaduri, S.S. Park, ACS Appl. Mater. Interfaces 7 (2015) 15506–15513.
[45] L.M.D.R.S. Martins, S.A.C. Carabineiro, J. Wang, B.G.M. Rocha, F.J. Maldonado-Hodar, A.J.L. Pombeiro, ChemCatChem 9 (2017) 1211–1221.
[46] M. Stratakis, H. Garcia, Chem. Rev. 112 (2012) 4469–4506.
[47] X. Liu, L. He, Y.-M. Liu, Y. Cao, Acc. Chem. Res. 47 (2013) 793–804.
[48] A. Buonerba, C. Cuomo, S.O. Sachez, P. Canton, A. Grassi, Chem. Eur J. 18 (2012) 709–715.
[49] B.N. Zope, D.D. Hibbitts, M. Neurock, R.J. Davis, Science 330 (2010) 74–78.